SciMedCentral

JSM

Biotechnology & Biomedical Engineering

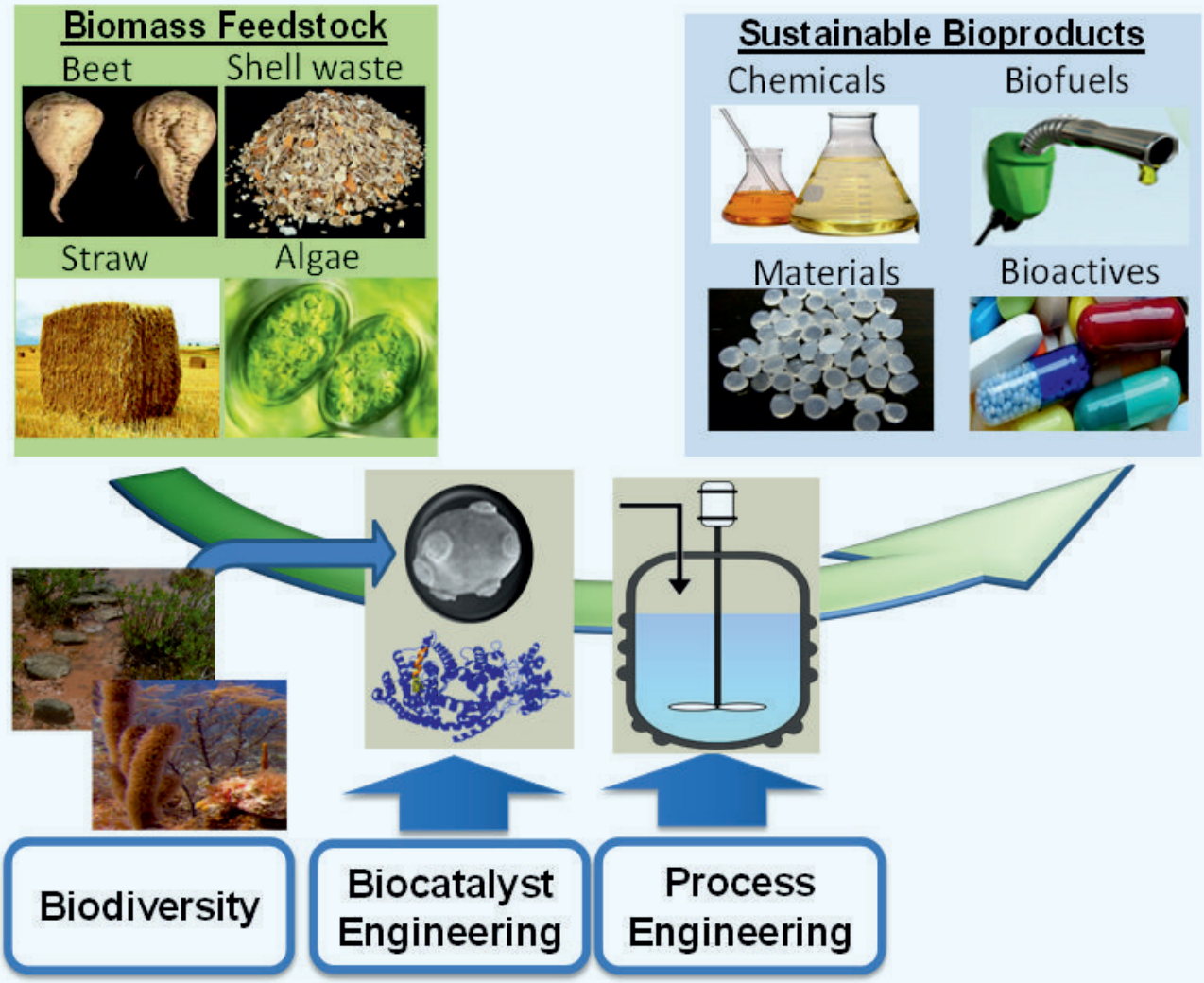

Special Issue on

Industrial Biotechnology-Made in Germany: The path from policies to sustainable energy, commodity and specialty products

Edited by:

Dr. Thomas Brück

Professor of Industrial Biocatalysis, Dept. of Chemistry, Technische Universität München (TUM), Germany

Research Article

A Novel Natural NADH and NADPH Dependent Glutathione Reductase as Tool in Biotechnological Applications

Reiter, J.[1,2], Pick, A.[1], Wiemann, L.O.[2], Schieder, D.[1] and Sieber, V.[1,2]*

[1]Chair of Chemistry of Biogenic Resources, Technische Universität München, Germany
[2]Fraunhofer IGB, Projektgruppe BioCat, Germany

***Corresponding author**
Prof.Dr. Volker Sieber, Chair of Chemistry of Biogenic Resources, Technische Universität München, Schulgasse 16, 94315 Straubing, Germany, Tel: 4909421187301; Email: sieber@tum.de

Submitted: 16 April 2014
Accepted: 12 May 2014
Published: 14 May 2014
ISSN: 2333-7117

Keywords
- Glutathione reductase
- NADH
- Allochromatium vinosum

Abstract

The antioxidant glutathione (GSH) is an important reducing agent in cell physiology. Glutathione reductases (GR) of humans and higher organisms convert oxidized glutathione (GSSG) to two reduced GSH molecules under consumption of the co-factor NADPH. GSH acts as an antioxidant eliminating reactive oxygen species in the cell. We found a novel GR being able to accept both NADPH and much cheaper NADH for GSSG reduction. For the first time we produced it in *E. coli* and purified active GR from *Allochromatium vinosum*, determined its K_m-values for NADH (0.026 mM) and NADPH (0.309 mM), as well as its temperature optimum (20 °C) and pH optimum (pH 8). Since numerous bio-diagnostic assays and enzymatic processes are dependent on GRs the possibility to use a cheaper co-substrate could help to overcome cost limitations in future.

ABBREVIATIONS

GR: Glutathione Reductase; GSH: Reduced Glutathione; GSSG: Oxidized Glutathione

INTRODUCTION

All organisms have developed certain mechanisms to cope with cellular stress caused by reactive oxygen species, pathogens, unfavorable temperature and environmental conditions or heavy metal–contaminations to name only a few [1-5]. Detoxification of reactive oxygen species or degradation of xenobiotics in living cells, for example, often involves reduced glutathione (GSH). For instance the ascorbate-glutathione cycle is part of the peroxide degradation process [5-8]. The GSH (γ-L-Glutamyl-L-cysteinyl-glycin tripeptide) has a mid-point redox potential of -318 mV. In addition, glutathione plays important roles in the cells' iron metabolism, DNA and protein synthesis as well as enzyme activation.

Furthermore, reduced glutathione is the substrate for various cellular metabolic pathways that finally oxidize glutathione, where two GSH molecules are linked by a disulfide bond. However, the most critical process in living cells is to maintain the balance between reduced and oxidized glutathione (GSSG) and that is permanently adjusted by glutathione reductases (GR) [5].

Glutathione reductases have found important applications in industrial as well as medical biotechnology. For example, glutathione reductase was recently used in an enzymatic multistep cascade for the deoxygenation of vicinal diol derivatives, by a hydrogen borrowing mechanism (Figure 1) [9]. This cascade has high potential for the defunctionalization of polyhydroxy compounds.

Moreover, several novel and highly sensitive detection methods for analyzing *in vivo* levels of glutathione and glutathione disulfide have been developed [10,11]. These methods are important for pharmacology as they allow the monitoring of oxidative stress, or to study cellular responses towards drugs and toxic compounds. Rahman setup a high throughput detection method for the GSH level by reducing GSH with 5,5'-dithio-bis (2-nitrobenzoic acid) (i.e. Ellman's reagent) yielding highly chromophoric 5-thio-2-nitrobenzoic acid [10] while Noh applied an electrochemical detection method for glutathione [11]. Both assays are based on the reduction of GSSG by a eukaryotic GR that only accepts NADPH. However, commercially available reduced β-Nicotinamide adenine dinucleotide is approximately ten times cheaper than reduced β-Nicotinamide adenine dinucleotide 2′-phosphate. Therefore, switching to NADH dependent assays could significantly decrease costs.

Glutathione reeducates [NAD(P)H: glutathione disulfide oxidoreductase, EC 1.8.1.7.] have been described in various plants, animals, fungi, yeasts and bacteria [12-17]. However, until now most GR's have been described as being strictly NADPH dependent. Though GRs from human erythrocyte and from Spinach were found to also utilize NADH, but the maximal reaction rates achieved here were only ca. 20 % of those obtained with NADPH [18-19]. So even though both enzymes are able to use NADH their main their main activity still lies with NADPH [20].

About 40 years ago a glutathione reductase from *Allochromatium vinosum* (reclassified, formerly known as *Chromatium vinosum*) had been purified and partially characterized and shown to be highly specific for NADH [21]. *Chromatiaceae* represent a very rudimentary bacterial group and it is assumed that this group developed its NADPH dependency later than its NADH-dependency [22]. Till date, there has been

no report about other natural glutathione reductases exhibiting a preference for NADH. Since just recently the genome of *Allochromatium vinosum* has been sequenced we now for the first time were able to clone and express an *E. coli* codon-optimized *avGR* gene and to purify and characterize the corresponding protein to make it available for potential applications in diagnostics and biotechnology where reduced cofactor costs are of advantage.

MATERIALS AND METHODS

Chemicals, strains and gene synthesis

All chemicals in this paper were purchased from Sigma-Aldrich (Germany). The *Allochromatium vinosum DSM 180* glutathione reductase YP_003443292 was synthesized with codon optimization for *Escherichia coli* by Life Technologies GmbH (Germany) in a pUC18 derivative. The open reading frame of the *av*GR gene fragment was cut out of this plasmid with *Bsa*I and *Psi*I and cloned with a C-terminal His-tag in a pET28b derivative (pCBR-C-His with a *Bsa*I and *Bfu*AI restriction site. Predigested with *Bsa*I, 3´sticky ends were filled with klenow fragment. In the next step the 5´ end was cut with *Bfu*AI, creating a *Bsa*I cloning site) (Novagen, Germany; NEB, U.S.). This plasmid was sequenced and used to transform *Escherichia coli* BL21 (DE3) (Merck KGaA, Germany). The protein was expressed in *Escherichia coli* BL21 (DE3). NADH and NADPH were purchased by Carl Roth (Germany).

Expression and purification

After expression in LB medium with 50 µg/mL kanamycin induced at OD_{600} = 0.8 by 1 mM IPTG at 37°C for 4 h the cells were harvested (4500 g, 4°C, 30 min) and applied to a cell disruptor (Constant Systems Ltd., U.S.) in binding buffer (Tris/HCl pH 7.2, 10% (v/v) glycerol, 20 mM imidazole). The cell extract was centrifuged (25,000 g, 4°C, 20 min), applied to a Ni^{2+}-NTA column (4 mL, GE, U.S.) and then fractionated in elution buffer (Tris/HCl pH 7.2, 10% (v/v) glycerol, 500 mM imidazole). The purity of elution fractions were tested by SDS-PAGE and Coomassie staining and protein concentrations were measured by Bradford (Roti Nanoquant, Carl Roth, Germany) [23]. The enzyme was stored in batch samples in the elution buffer (20% glycine, 500 mM imidazole, pH 6.5) at -20°C, single fractions of 3700 µg/mL protein concentration were gently thawed directly before starting an activity assay, diluted 1:20,000. A slight activity loss of 10 to 20 % occurred on refreezing. Else, the enzyme was stable at 20°C.

Assay conditions

Activity of the enzyme was measured photometrically at 340 nm in 96 well plates. The assay was started by adding 7 mM GSSG (Sigma Aldrich, Germany) and 0.5 mM NADH or NADPH (Carl Roth, Germany) in a citrate-borate-phosphate (CBP) universal pH buffer (Carl Roth, Germany) to a solution of *av*GR in the same buffer. Temperature and pH dependence were measured in a universal pH 4-12 CBP buffer system.

For determining K_m and k_{cat} for NADH and NADPH activity measurements at optimal conditions (pH 8, 20 °C) and constant GSSG (7 mM) were performed. The concentration of NADH and NADPH was varied between 0.3 µM and 1 mM. K_m and k_{cat} for GSSG was determined in the presence of 1 mM NADH. Calculation of the kinetic constants was performed with Sigma Plot 11.0. Samples which contained NADH/NADPH concentrations above 1 mM were diluted before measurement.

Inhibition tests

Tests with flavin adenine dinucleotide (FAD) or GSSG pre-incubation prior to the assay were conducted with 0.5 mM FAD (Carl Roth, Germany) or 7 mM GSSG (Sigma Aldrich, Germany) following the above standard assay protocol with CBP-buffer pH 8 at 20 °C. Different ion concentrations on GR were tested with 5 mM and 10 mM NaCl, Na_2SO_4 and Na_3PO_4 following the above standard protocol under optimum conditions.

Structure modeling

A structure model for *av*GR was created using Phyre2 [24].

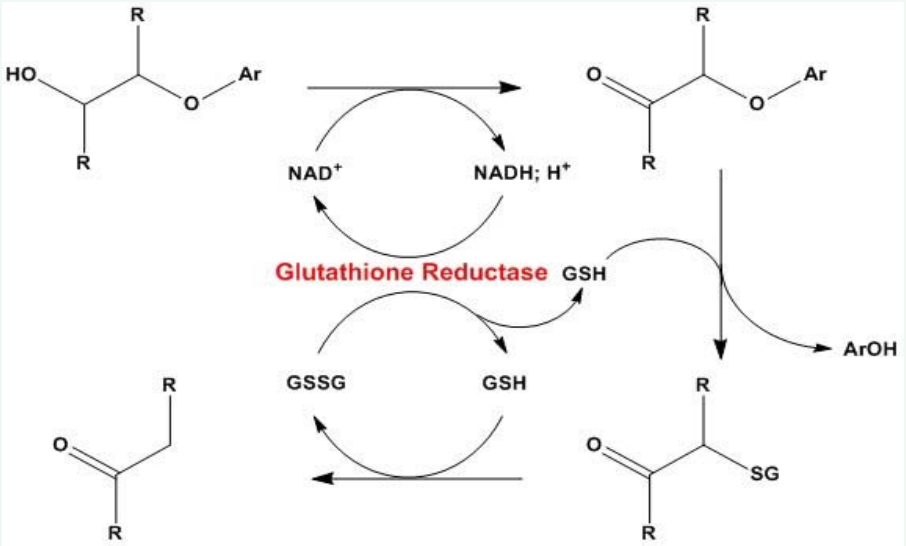

Figure 1 Enzymatic multistep cascade for the enzymatic deoxygenation of vicinal diol derivatives by a hydrogen borrowing mechanism [9].

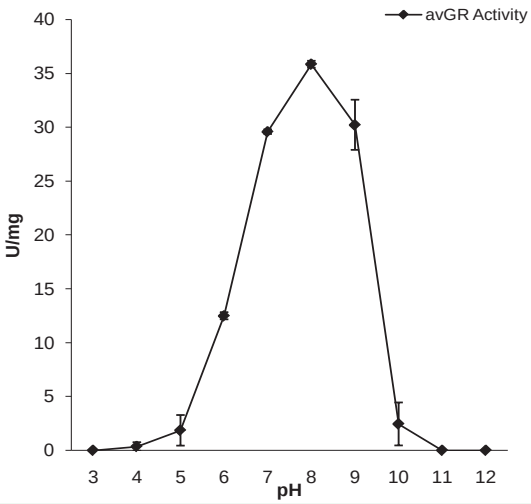

Figure 2 Reaction of *av*GR at 340 nm with 0.5 mM NADH and 7 mM glutathione in CBP-buffer pH 4-11. (n=3).

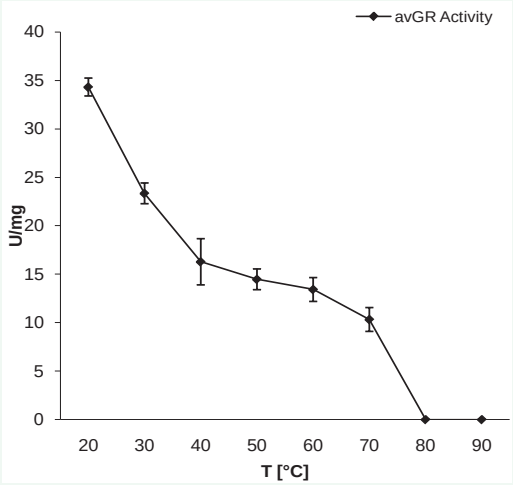

Figure 3 Temperature-related *av*GR activity with 0.5 mM NADH and 7 mM glutathione in CBP-buffer pH8 at 340 nm, measured between 20 °C and 90 °C (n=3).

Table 1: Activity of *av*GR towards different substrates compared to control experiment (%). (n=3).

K = 100%	5 mM	10 mM
NaCl	40.4 ± 1.9	63.3 ± 16.8
Na_2SO_4	106.7 ± 13.3	111.1 ± 10.2
Na_3PO_4	97.8 ± 10.2	117.8 ± 7.7

Abbreviations: *av*GR *Allochromatium vinosum* glutathione reductase; NaCl Sodium chloride; Na_2SO_4 Sodium sulfate; Na_3PO_4 Sodium phosphate

Table 2: Activity of *av*GR with 0.5 mM NADH, 0.5 mM oxidized glutathione in CBP-buffer pH 8 after pre-incubation of the enzyme with FAD or GSSG. (n=3).

	*av*GR	*av*GR +FAD	*av*GR + GSSG
%	100	194.2 ± 14.2	105.4 ± 8.1

Abbreviations: *av*GR *Allochromatium vinosum* glutathione reductase; FAD Flavin adenine dinucleotide; GSSG oxidized glutathione; NADH Nicotine adenine dinucleotide; CBP Citrate borate phosphate buffer.

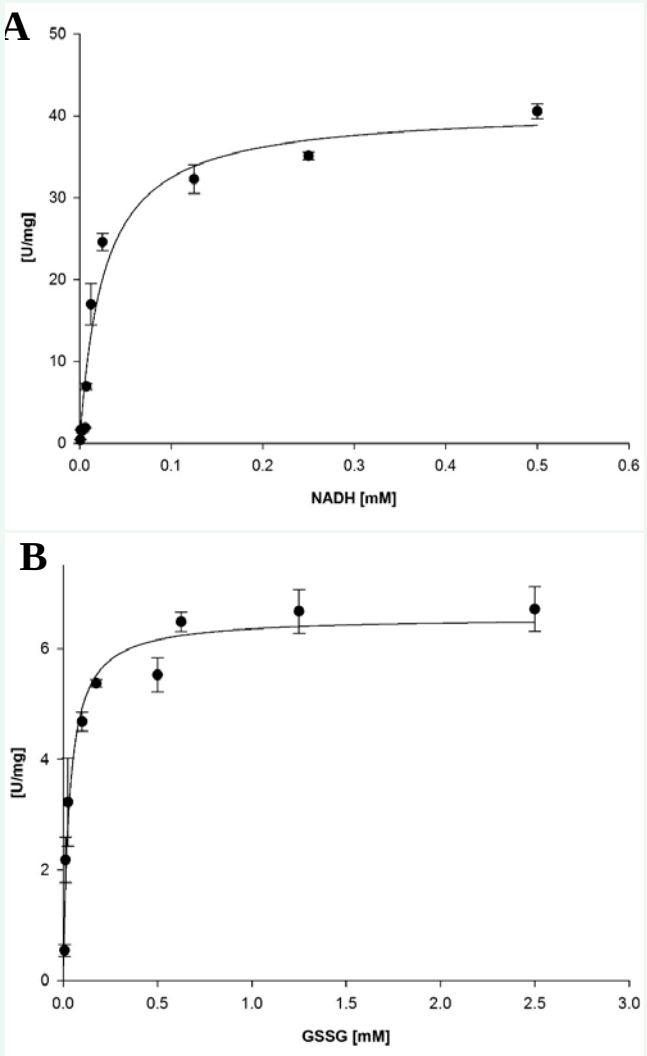

Figure 4 (A) *av*GR kinetic under variation of NADH concentrations, and (B) oxidized glutathione concentrations in CBP-buffer pH 8, 20 °C as triplicates.

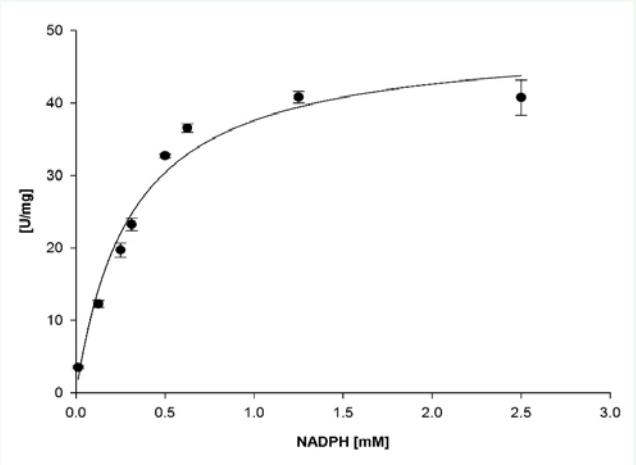

Figure 5 *av*GR kinetic under variation of NADPH in CBP-buffer pH 8, 20 °C (n=3).

Subsequently, the derived model was used for 3DLigandSite to integrate FAD and NADH into the structure [25]. Out of a set of different FAD and NADH/NADPH molecules respectively one candidate was chosen and the remaining removed from the model. In a final step the model was compared to crystal structures of glutathione reductase from *E. coli* (PDB: 1 GER and 1 GEU) as well as a variant thereof with improved acceptance of NADH.

RESULTS AND DISCUSSION

We were able to annotate the gene function to a glutathione reductase in *Allochromatium vinosum DSM 180.* We postulated the gene YP_003443292 coding for a 458aa predicted glutathione reductase of the sequenced genome of *Allochromatium vinosum DSM 180* to be responsible for the GR activity described 40 years ago in this organism [21]. The gene was codon optimized for *E. coli* and cloned with a His-tag. Soluble protein was expressed by *E. coli BL21 (DE3)* in LB-media and purified via a metal-chelate column (GE, U.S.). Protein content of the elution peak fractions varied between 3700 µg/mL and 4700 µg/mL and the SDS-PAGE showed clear single bands at 48.8 kDa (data not shown).

We were able to express the soluble *av*GR enzyme with codon optimization in *E.coli* and were able to purify the His-tagged protein in an active form as well. In all assays *av*GR was pre-incubated for 5 min with FAD. The external addition of FAD is supposed to replenish potentially lost flavin adenine dinucleotide from the enzymes active center during the purification process. The reaction was started with 0.5 mM NADH and 7 mM GSSG. The pH dependence of *av*GR activity was tested in citrate-borate-phosphate buffer (CBP) ranging from pH 4-12. The optimum for *av*GR was determined to be 35.8 ± 0.3 U/mg at pH 8, thus being above the published pH of 7 for the native enzyme (Figure 2).

This is important as earlier described applications [9,10,11] all use slightly alkaline conditions. The temperature optimum for *av*GR was investigated in the range from 20 °C to 90 °C at pH 8 and was determined to be 34.3 ± 1.5 U/mg at 20 °C (Figure 3).

Previous studies showed an inhibition or activation of native *av*GR by salts like phosphate [21]. We tested the inhibition of recombinant *av*GR activity at its optimal conditions by addition of different concentrations of NaCl, Na_2SO_4, and Na_3PO_4. The activity was measured photometrically at 340 nm. Whereas 5 mM NaCl decreased activity of *av*GR by ca. 60 %, activity in phosphate increased 17.8 ± 7.7 % at 10 mM Na_3PO_4. This result stands in contrast to those obtained previously for the native enzyme and it is important when considering its potential applications in commonly used phosphate buffers (Table 1).

Chung observed an inhibition of the *Allochromatium vinosum* reductase by pre-bound GSSG and proposed to alleviate this by pre-incubation of *av*GR with FAD. We found almost no difference by GSSG pre-incubation, but an almost-twofold increase of activity with FAD pre-incubation to about 194.2 ± 14.2 % (Table 2) [21].

K_m and k_{cat} were determined photometrically following the decline of NADH at different concentrations. The concentrations of *av*GR and GSSG (7 mM) were kept constant and reactions were run at pH 8 and 20 °C. The K_m for NADH and NADPH were identified as 0.026 **±** 0.004 mM (Figure 4A) and 0.309 **±** 0.030 mM respectively. (Figure 5) The k_{cat} values were 33.23 ± 1.23 s^{-1} and

```
avGR   1    MSQHFDLIAIGGGSGGLAVAEKAAQFGRRVALIEGAKLGGTCVNAGCVPKKVMWYAANLA  60
            M++H+D IAIGGGSGG+A   +AA +G++ ALIE  +LGGTCVN GCV KKVMW+AA +
ecGR   1    MTKHYDYIAIGGGSGGIASINRAAMYGQKCALIEAKELGGTCVNVGCVQKKVMWHAAQIR  60

avGR   61   AAV-ADAPDYGIQARSDGLDWGKLIAGRNQYIADINGYWDGYAERLGLTRIDGFARFVDA  119
             A+    PDYG     +  +W  LIA R  YI  I+  ++    +  +  I GFARFVDA
ecGR   61   EAIHMYGPDYGFDTTINKFNWETLIASRTAYIDRIHTSYENVLGKNNVDVIKGFARFVDA  120

avGR   120  RTVAVGDQHYTADHIVIATGGRPIVPRMPGAELGITSDGFFALEEQPKRVAIIGGGYIGV  179
            +T+ V  +  TADHI+IATGGRP  P +PG E GI SDGFFAL   P+RVA++G GYI V
ecGR   121  KTLEVNGETITADHILIATGGRPSHPDIPGVEYGIDSDGFFALPALPERVAVVGAGYIAV  180

avGR   180  ELAGVLSALGTEITIVAIEDRMLALFDPLISETLAENMTLHGIDMHLQFEVAGIERDEQG  239
            ELAGV++ LG +  +   +   L  FDP+ISETL E M   G  +H       + ++  G
ecGR   181  ELAGVINGLGAKTHLFVRKHAPLRSFDPMISETLVEVMNAEGPQLHTNAIPKAVVKNADG  240

avGR   240  -LVLAARDGQRLTGFDQVIWAVGRAPNTRELNLEAAGITVERSGVIPTDAWQNTTVPGIY  298
             L L   DG+  T  D +IWA+GR P    +NLEAAG+     G I  D +QNT + GIY
ecGR   241  SLTLELEDGRSET-VDCLIWAIGREPANDNINLEAAGVKTNEKGYIVVDKYQNTNIEGIY  299

avGR   299  AIGDITGREPLTPVAIAAGRRLAERLFNDKPDSKLDYENVPTVVFAHPPIGKVGLTEPEA  358
            A+GD TG   LTPVA+AAGRRL+ERLFN+KPD  LDY N+PTVVF+HPPIG VGLTEP+A
ecGR   300  AVGDNTGAVELTPVAVAAGRRLSERLFNNKPDEHLDYSNIPTVVFSHPPIGTVGLTEPQA  359

avGR   359  RERYG-DTLTIYETSFTPMRYALNAHGPKTAMKLVCAGEDEKVVGIHLIGDGVDEMMQGF  417
            RE+YG D + +Y++SFT M  A+  H     MKLVC G +EK+VGIH IG G+DEM+QGF
ecGR   360  REQYGDDQVKVYKSSFTAMYTAVTTHRQPCRMKLVCVGSEEKIVGIHGIGFGMDEMLQGF  419

avGR   418  GVAVKMGATKADLDNTVAIHPCSAEELVTLK  448
             VA+KMGATK D DNTVAIHP +AEE VT++
ecGR   420  AVALKMGATKKDFDNTVAIHPTAAEEFVTMR  450
```

Figure 6 Alignment of *av*GR and *ec*GR with glycine 178 and glutamate 198 (red boxes) of the NADH binding sites of pyridine dinucleotide oxidoreductases (Basic Logarithmic Alignment Search Tool, BLAST).

40.02 ± 1.46 s^{-1}respectively. K_m and k_{cat} for GSSG with constant NADH at 0.5 mM were 0.033 ± 0.007 mM and 5.34 ± 1.47 s^{-1} (Figure 4B).

Intensive research of glutathione reductases has been conducted not only to elucidate its role in cell physiology but also to understand the mechanism of cofactor acceptance. A comparison of *Homo sapiens* GR and *Plasmodium falciparum* GR (*pf*GR) showed up to 5 % activity of *pf*GR and *hs*GR towards NADH and a lower K_m value of *pf*GR for NADPH compared to *hs*GR [26]. Moreover, wild type *Escherichia coli* GR (*ec*GR) shows a strongly decreased activity of around 5 % with NADH. As a result of the crystal structure for *hs*GR and the high homology towards *ec*GR first mutagenesis studies were carried out. Scrutton were successful in the redesign of the coenzyme specificity of *ec*GR [27]. As a member of the flavoprotein disulphide oxidoreductase family glutathione reductase shares some typical features found in enzymes interacting with pyrophosphate moieties (Figure 6) [26].

The unique βαβ-fold responsible for the ADP binding of the cofactor carries a GxGxxG/A motif [28]. Scrutton suspected that the differentiation between glycine and alanine in the third position is correlated with the preference towards NADH or NADPH [27]. But a more intense study by Carugo and Argos on basis of crystal structures of different enzymes did not reveal any significant correlation for this feature [29]. A clear characteristic to distinguish between the two pyridine nucleotide cofactors is the residue at the C-terminal end of the second β-strand. It is negatively charged when a hydrogen bond to the 2'-hydroxyl group of NADH is required and in most cases hydrophobic for the 2'-phosphate of NADPH [30]. Within the study of Scrutton et al. for *ec*GR a change in these characteristic residues allowed a complete switch towards NADH by lowering the K_m from 2 mM to 0.086 mM. The catalytic efficiency k_{cat}/K_m was increased by a factor of 72 (24.4 min^{-1} μM^{-1}) compared to the wild type with 0.34 min^{-1} μM^{-1}. Based on this information the homology model as well as the amino acid sequence was compared to characterized glutathione reductases. The characteristic glycine residue (AS 178) found for enzymes preferring NADH as well as a negatively charged residue at the end of the β-strand (AS 198) can be found in *av*GR. Glutamate at position 198 is the main factor influencing the binding of NADPH by decreasing the space for the 2'phosphate and preventing stabilization. (Figure 7)

These structural features correspond to the measured kinetic parameters and the observed preference for NADH. Glutathione reductase from *Allochromatium vinosum* is still superior against the variant of *ec*GR in context of K_m (three times lower) and also for k_{cat}/K_m which is with 76.6 min^{-1} μM^{-1} three times higher. The NADH attachment site is within a larger FAD binding domain. Huber and Brandt (1980) calculated glutathione reduction in human glutathione reductase with the following three steps, (**1**) NADPH binding (>300 s^{-1}) (**2**) hydride transfer to FAD (153 s^{-1}) and (**3**) disulfide reduction by FAD (68 s^{-1}) [31]. In a binding study for NADH, Y197 played an important role in the catalytic mechanism by opening and blocking the binding pocket of NADH/NADPH and it is also conserved in *av*GR. K66 and E201 of *hs*GR transfer the hydride by forming an ion pair whereas oxygen atoms of E201 are closer to NADH than K66 nitrogen atoms, implicating that the carboxyl group seems to be more important. Both sites are conserved in the NADH/NADPH binding pockets of glutathione and mercury reductases or liponamide dehydrogenases [31-36]. However, only crystallization and detailed binding studies could clearly elucidate the exact mechanism of *av*GR as NADH and NADPH dependent glutathione reductase.

CONCLUSION

The availability of enzymes that are using the cheapest possible cofactor is essential for cost effective biocatalysis. In making this rare NADH-dependent GR available as recombinant enzyme in *E.coli* we provided a new tool for GR dependent diagnostic assays or for GSH dependent biotransformation reactions. *av*GR has a

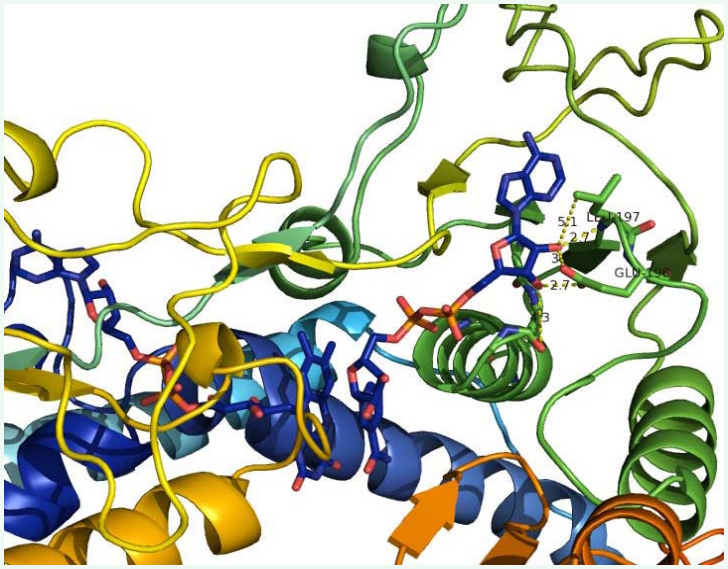

Figure 7 Structure model of *av*GR with FAD and NAD^+. Residues leucine 197 and glutamate 198 are shown in the stick mode and the distances to the 2' and 3'-hydroxy groups of the ribose ring are specified.

superior catalytic efficiency than previously engineered GR from *E. coli*. The enzyme can be produced in soluble form in good yield. Storage stability is high. At temperature above 20 °C the enzyme has reduced activity. However, even at 70 °C significant activity was still available showing that the enzyme can be used at higher temperature. Recently we demonstrated the application of this enzyme in a redox-neutral synthetic enzymatic pathway for the degradation of lignin [9]. In future it could even be feasible to couple this NADH-dependent GR with important toxic or environmentally problematic industrial waste degradation approaches.

ACKNOWLEDGEMENT

We would like to thank Kerstin Stadler and Benjamin Kick for experimental support. We also thank the Bavarian government for funding this project within the BayernFit program.

REFERENCES

1. Foyer CH, Noctor G. Ascorbate and glutathione: the heart of the redox hub. Plant Physiol. 2011; 155: 2-18.
2. Noctor G, Mhamdi A, Chaouch S, Han Y, Neukermans J, Marquez-Garcia B, et al. Glutathione in plants: an integrated overview. Plant Cell Environ. 2012; 35: 454-484.
3. Meyer AJ, Hell R. Glutathione homeostasis and redox-regulation by sulfhydryl groups. Photosynth Res. 2005; 86: 435-457.
4. Parisy V, Poinssot B, Owsianowski L, Buchala A, Glazebrook J, Mauch F. Identification of PAD2 as a gamma-glutamylcysteine synthetase highlights the importance of glutathione in disease resistance of Arabidopsis. Plant J. 2007; 49: 159-172.
5. Hicks LM, Cahoon RE, Bonner ER, Rivard RS, Sheffield J, Jez JM. Thiol-based regulation of redox-active glutamate-cysteine ligase from Arabidopsis thaliana. Plant Cell. 2007; 19: 2653-2661.
6. May MJ, Leaver CJ. Oxidative Stimulation of Glutathione Synthesis in Arabidopsis thaliana Suspension Cultures. Plant Physiol. 1993; 103: 621-627.
7. Xiang C, Werner BL, Christensen EM, Oliver DJ. The biological functions of glutathione revisited in arabidopsis transgenic plants with altered glutathione levels. Plant Physiol. 2001; 126: 564-574.
8. Mullineaux PM, Rausch T. Glutathione, photosynthesis and the redox regulation of stress-responsive gene expression. Photosynth Res. 2005; 86: 459-474.
9. Reiter J, Strittmatter H, Wiemann LO, Schieder D, Sieber V. Enzymatic cleavage of lignin ß-O-4 aryl ether bonds via net internal hydrogen transfer. Green Chem. 2013; 15: 1373- 1381.
10. Rahman I, Kode A, Biswas SK. Assay for quantitative determination of glutathione and glutathione disulfide levels using enzymatic recycling method. Nat Protoc. 2006; 1: 3159-3165.
11. Noh HB, Chandra P, Moon JO, Shim YB. In vivo detection of glutathione disulfide and oxidative stress monitoring using a biosensor. Biomaterials. 2012; 33: 2600-2607.
12. Prast-Nielsen S, Huang HH, Williams DL. Thioredoxin glutathione reductase: its role in redox biology and potential as a target for drugs against neglected diseases. Biochim Biophys Acta. 2011; 1810: 1262-1271.
13. Johann L, Lanfranchi DA, Davioud-Charvet E, Elhabiri M. A physico-biochemical study on potential redox-cyclers as antimalarial and anti-schistosomal drugs. Curr Pharm Des. 2012; 18: 3539-3566.
14. Backos DS, Franklin CC, Reigan P. The role of glutathione in brain tumor drug resistance. Biochem Pharmacol. 2012; 83: 1005-1012.
15. Krauth-Siegel RL, Leroux AE. Low-molecular-mass antioxidants in parasites. Antioxid Redox Signal. 2012; 17: 583-607.
16. Mendoza-Cózatl D, Loza-Tavera H, Hernández-Navarro A, Moreno-Sánchez R. Sulfur assimilation and glutathione metabolism under cadmium stress in yeast, protists and plants. FEMS Microbiol Rev. 2005; 29: 653-671.
17. López-Mirabal HR, Winther JR. Redox characteristics of the eukaryotic cytosol. Biochim Biophys Acta. 2008; 1783: 629-640.
18. Scott EM, Duncan IW, Ekstrand V. Purification and Properties of Glutathione Reductase of Human Erythrocytes. J Biol Chem. 1963; 238: 3928-3933.
19. Vanoni MA, Wong KK, Ballou DP, Blanchard JS. Glutathione reductase: comparison of steady-state and rapid reaction primary kinetic isotope effects exhibited by the yeast, spinach, and Escherichia coli enzymes. Biochemistry. 1990; 29: 5790-5796.
20. Perham RN, Scrutton NS, Berry A. New enzymes for old: redesigning the coenzyme and substrate specificities of glutathione reductase. Bioessays. 1991; 13: 515-525.
21. Chung YC, Hurlbert RE. Purification and properties of the glutathione reductase of Chromatium vinosum. J Bacteriol. 1975; 123: 203-211.
22. Horocker BL. [Alternate pathways of carbohydrate metabolism and their physiological significance]. Seikagaku. 1965; 37: 313-324.
23. Bradford MM. A rapid and sensitive method for the quantitation of microgram quantities of protein utilizing the principle of protein-dye binding. Anal Biochem. 1976; 72: 248-254.
24. Kelley LA, Sternberg MJ. Protein structure prediction on the Web: a case study using the Phyre server. Nat Protoc. 2009; 4: 363-371.
25. Wass MN, Kelley LA, Sternberg MJ. 3DLigandSite: predicting ligand-binding sites using similar structures. Nucleic Acids Res. 2010; 38: W469-473.
26. Krauth-Siegel RL, Müller JG, Lottspeich F, Schirmer RH. Glutathione reductase and glutamate dehydrogenase of Plasmodium falciparum, the causative agent of tropical malaria. Eur J Biochem. 1996; 235: 345-350.
27. Scrutton NS, Berry A, Perham RN. Redesign of the coenzyme specificity of a dehydrogenase by protein engineering. Nature. 1990; 343: 38-43.
28. Wierenga RK, Terpstra P, Hol WG. Prediction of the occurrence of the ADP-binding beta alpha beta-fold in proteins, using an amino acid sequence fingerprint. J Mol Biol. 1986; 187: 101-107.
29. Carugo O, Argos P. NADP-dependent enzymes. I: Conserved stereochemistry of cofactor binding. Proteins. 1997; 28: 10-28.
30. Schierbeek AJ, Swarte MB, Dijkstra BW, Vriend G, Read RJ, Hol WG, et al. X-ray structure of lipoamide dehydrogenase from Azotobacter vinelandii determined by a combination of molecular and isomorphous replacement techniques. J Mol Biol. 1989; 206: 365-379.
31. Wierenga RK, De Maeyer MH, Hol WJ. Interaction of pyrophosphate moieties with alpha-helixes in dinucleotide-binding proteins. Biochemistry. 1985; 24: 1346-1357.
32. Sarma GN, Savvides SN, Becker K, Schirmer M, Schirmer RH, Karplus PA. Glutathione reductase of the malarial parasite Plasmodium falciparum: crystal structure and inhibitor development. J Mol Biol. 2003; 328: 893-907.
33. Karplus PA, Schulz GE. Substrate binding and catalysis by glutathione reductase as derived from refined enzyme: substrate crystal structures at 2 A resolution. J Mol Biol. 1989; 210: 163-180.

34. Bump EA, Taylor YC, Brown JM. Role of glutathione in the hypoxic cell cytotoxicity of misonidazole. Cancer Res. 1983; 43: 997-1002.

35. Rice DW, Schulz GE, Guest JR. Structural relationship between glutathione reductase and lipoamide dehydrogenase. J Mol Biol. 1984; 174: 483-496.

36. Huber PW, Brandt KG. Kinetic studies of the mechanism of pyridine nucleotide dependent reduction of yeast glutathione reductase. Biochemistry. 1980; 19: 4569-4575.

Cite this article

Reiter J, Pick A, Wiemann LO, Schieder D, Sieber V (2014) A Novel Natural NADH and NADPH Dependent Glutathione Reductase as Tool in Biotechnological Applications. JSM Biotechnol Bioeng 2(1): 1028.